Polymer 53 (2012) 3498–3507

Contents lists available at SciVerse ScienceDirect

Polymer

journal homepage: www.elsevier.com/locate/polymer

Synthesis and characterization of a new polymer–drug conjugate with pH-induced activity

Hui-Ping Chang [1], Jian-Ying Chen, Pei-Shan Zhong, Yung-Hsien Chang, Mong Liang*

Department of Applied Chemistry, National Chiayi University, Chiayi 60004, Taiwan, Republic of China

ARTICLE INFO

Article history:
Received 17 April 2012
Received in revised form
26 May 2012
Accepted 4 June 2012
Available online 13 June 2012

Keywords:
Polymer–drug
Tumor-specific targeting
Stimuli-responsive

ABSTRACT

A well-defined, stimuli-responsive tetrapolymer with pH-responsive characteristics and targeting specificity has been synthesized by radical copolymerization of methacrylic acid, *N*-(2-hydroxypropyl)methacrylamide, methacryloyl glycylglycyl sulfamethoxazole, and *N*-(methacryloyl)glycylglycine 4-nitrophenyl ester. The structure and properties of tetrapolymer were investigated by NMR, FT-IR, UV–visible absorption, TEM and gel permeation chromatography. Incorporation of maleimide linker into tetrapolymer facilitates its conjugation with antibody fragments, as demonstrated by the solid-phase immunoassay experiments. The TEM image shows that tetrapolymer had self-assembled a spherical micelle with a diameter ranging from 50 to 150 nm. Altering the pH of the solution leads to a different extent of aggregation at pH 6.5–3.5, responding in accordance with the properties associated with the extracellular environment of solid tumors and endocytosis. Furthermore, fluorescence spectroscopy indicated a critical micelle concentration (CMC) of 1 mg/mL. Because of the solvation and ionization effects, the tetrapolymer showed considerably enhanced antibacterial activities against *Escherichia coli* in the presence of DMSO and the antibacterial activity increased with decreasing pH value.

1. Introduction

The application of water-soluble polymer–drug conjugate for anti-cancer drug delivery represents a promising approach to cancer therapy. The main benefits of using these macromolecular therapeutics include: (1) improved drug accumulation in tumor cells because of the enhanced permeability and retention (EPR) effect [1]; (2) lower drug doses, thereby reducing non-specific toxicity to healthy organs [2]; and (3) contributing to the development of a site-specific drug that targets the tumor site to maximize the efficiency and allows the creation of a programmed profile of drug release [3]. Polymer–drug conjugate generally consists of a water-soluble polymer containing drug molecules and bioactive moieties in its side chains to ensure not only the site-specific targeting of the pathological area, but also the modulation of pharmacokinetics of the drug carrier. Significant progress has been made in the design and synthesis of various polymer–drug conjugates [4–10]. Some studies have focused on designing macromolecular drug delivery systems by using the EPR effect for tumor-seeking anti-cancer agents [11–14]. However, in cases where the EPR effect is not operative (e.g., smaller tumors), several site-specific drug delivery systems have been designed. Here, the antibody acts as a homing device by attaching it to the reactive polymer precursors [15–18]. Alternatively, it can be modified with polymerizable groups, and then undergoes copolymerization with water-soluble comonomers [19,20]. The use of such targeting moiety not only reduces adverse side effects by allowing the drug to be delivered to the specific site of action, but also facilitates cellular uptake of the drug by receptor-mediated endocytosis. Active targeting ligands such as monoclonal antibodies [21,22], folates [23,24], transferrin [25,26], and luteinizing hormone-releasing hormone [27] have shown to be effective in delivering drugs to tumor cells. However, because of the absence of a substantial improvement in clinical applications, a more efficient strategy for designing anti-cancer drugs that exhibit a high selectivity to tumor tissues must be developed. It is thought that a combination of both active and passive targeting ligands may produce synergistic effects and has higher efficiency than each targeting ligands separately. By using a local stimuli characteristic of the pathological site, an additional selectivity and drug accumulation could be gained if these functional moieties were to be incorporated into the drug carrier. Temperature and pH conditions are 2 most commonly used stimuli for this purpose. Compared with the normal physiological pH level of 7.4, the extracellular environment of solid tumors is slightly acidic, with a pH level of 6.8 dropping between 5 and 6 in endosomes or between 4 and 5 in

* Corresponding author. Fax: +886 52717901.
E-mail address: mliang@mail.ncyu.edu.tw (M. Liang).
[1] Current address: St. Martin De Porres Hospital, Chiayi, Taiwan.

0032-3861/$ – see front matter © 2012 Elsevier Ltd. All rights reserved.
http://dx.doi.org/10.1016/j.polymer.2012.06.006

lysosomes after endocytosis [28,29]. TAT peptide-mediated polymeric micelles, which target tumor areas and are able to internalize into cells, were applied in the studies on the design of a pH-sensitive drug carrier in response to the change of external pH [30–34]. It has also been reported that drugs bound to a thiolated protein carrier or serum albumin through acid-sensitive linkers exhibited greater anti-cancer activity in animal tumor models than in free drugs [35–38]. Despite extensive research efforts, linear, drug-loaded, antibody-bearing and pH-responsive polymer conjugates remain a great challenge to synthetic chemists and may have potential applications in biomedicine.

The aim of this study is to synthesize a novel polymer–drug conjugate that would have both pH-responsive and bio-selective sensors for drug delivery systems. For this purpose, we conjugated sulfamethoxazole (SMX) as a model drug to the polymer side chain, testing the antimicrobial activity against *Escherichia coli* (*E. coli*). The drug was chosen not only for its nucleophilic reactivity toward the monomer containing 4-nitrophenoxy reactive groups, but also for its characteristic absorption peaks of oxazole in ^{1}H NMR spectroscopy, which allowed a precise determination of molar composition of the drug. It is assumed that a number of potential, primary amine-containing antitumor drugs (e.g., doxorubicin, cladribine, idarubicin, epirubicin, and gemcitabine) could also be attached to the polymer backbone in a similar manner, increasing tumor-targeting capabilities when combined with relevant cancer cells.

2. Experimental

2.1. Materials

2,2′-Azobis-isobutyronitrile (AIBN, Showa) was recrystallized in ethanol before use. Methacrylic acid (MAA, Showa) was purified by distillation and stored under N_2 prior to use. Tetrahydrofuran (THF), ethyl ether (Et_2O) were purchased from J. T. Baker. *N*-(2-Hydroxypropyl)methacrylamide (HPMA) was prepared according to a known procedure [39]. Methacryloyl chloride was obtained from TCI. Glycylglycine and di-*tert*-butyl dicarbonate ($(Boc)_2O$) were purchased from Alfa Aesar. *p*-Nitrophenol, 1,4-diaminobutane and trifluroacetic acid (TFA) were purchased from Acros. *N*,*N*′-Dicyclohexylcarbodiimide (DCC) and sulfamethoxazole (SMX) were purchased from Fluka. 3,3′,5,5′-Tetramethylbenzidine (TMB), albumin from bovine serum (BSA) were purchased from Sigma. Luria-Bertani (LB) broth was obtained from Lab M Limited. Pan CEA (H-8): sc-48364 mouse monoclonal IgG1 and goat anti-mouse IgG1-HRP (sc-2060) was obtained from Santa Cruz Biotechnology. *E. coli* (DH5) was purchased from GeneMark, Taicuung, Taiwan.

2.2. Characterization

^{1}H spectra were recorded on a 300 MHz Varian–Mercury$^+$300 spectrometer using deuterated solvent. FT-IR spectra were measured using a Shimadzu 8400 spectrophotometer. Gel permeation chromatography (GPC) was carried out using a DMF eluent that contained 0.05 mol L^{-1} LiBr at 80 °C at a flow rate of 0.8 mL/min^{-1}. Narrowly distributed poly(methyl methacrylate) standards in the molecular weight range of 2500–520,000 g mol^{-1} (Polymer Standards Service, USA) were utilized for calibration. Prior to GPC analysis, the polymers were modified by methylation of the carboxylic acid groups using trimethylsilyldiazomethane in DMF [40,41]. TEM measurements were carried out on a JEOL JEM-2100 electron microscope operated at an acceleration voltage of 100 kV. Polymer **1** solutions (1 mg/mL) containing 0.05 wt.% phosphotungstic acid were dropped onto the carbon-coated copper grids and then allowed to dry in air at room temperature before observation. Fluorescence measurements were performed on a Shimatsu F-7000 FL Spectrophotometer. Ultraviolet (UV) spectroscopy and optical transmittance of the aqueous polymer solutions (1 mg/mL) were recorded by JASCO V-630 spectrophotometer. The pH of the test solutions was controlled by adding tris(hydroxymethyl)aminomethane or phosphoric acid from 9 to 3.

2.3. Synthesis

2.3.1. Synthesis of N-methacryloyl glycylglycyl sulfamethoxazole (MA-GG-SMX)

N-methacryloylglycylglycine 4-nitrophenyl ester (MA-GG-ONp) was synthesized according to a literature protocol by the reaction of methacryloyl chloride with glycylglycine followed by esterification with *p*-nitrophenol in the presence of DCC [42]. Then, to a stirred solution of MA-GG-ONp (0.64 g, 2.0 mmol) in anhydrous DMF (4 mL) under nitrogen, sulfamethoxazole (SMX) (0.56 g, 2.2 mmol) was added. The reaction mixture was heated to 110 °C for 24 h. The solvent was removed under high vacuum and the resulting residue was purified by dissolving in a minimum amount of acetone and re-precipitated in ethyl ether solution. The product was collected as a brown powder and dried under vacuum for overnight (0.52 g, yield: 60%). ^{1}H NMR (DMSO-d_6) δ: 1.86 (s, 3H, CH_2=CH(CH_3)–), 2.28 (s, 3H, –CH_3 of oxazole unit), 3.76 (d, 2H, –NH–CH_2–CONHR–, J = 6.0 Hz), 3.92 (d, 2H, –CONH–CH_2–CONHAr–, J = 5.7 Hz), 5.36 (s, 1H, *trans* CH_2=C(CH_3)–), 5.74 (s, 1H, *cis* CH_2=C(CH_3)–), 6.09 (s, 1H, –*H* of oxazole ring), 7.78 (s, 4H, Ar–*H*), 8.27 (m, –NH), 10.19 (s, –NH). ^{13}C NMR (DMSO-d_6) δ: 11.82, 18.47, 42.41, 43.00, 94.99, 119.13, 120.11, 127.93, 133.21, 139.46, 142.78, 157.25, 167.90, 168.49, 169.47, 170.25, 171.22. IR (KBr) ν (cm^{-1}): 3358 (N–H), 3287 (N–H), 3115 (C–H), 3071 (C–H), 2984 (C–H), 2925 (C–H), 1718 (C=O), 1674 (C=O), 1648 (C=O), 1529 (C=C), 1324 (S=O asym), 1160 (S=O sym). Elemental analysis: calcd for $C_{18}H_{21}N_5O_6S$: C 49.60, H 4.80, N 16.00, S 7.30; found: C 49.07, H 5.00, N 15.43, S 7.08.

2.3.2. Synthesis of poly(MAA-co-HPMA-co-MA-GG-SMX-co-MA-GG-ONp) (*1*)

To a mixture of 0.045 g of HPMA (0.32 mmol), 0.05 g of MA-GG-ONp (0.16 mmol), 0.068 g of MA-GG-SMX (0.16 mmol) and 0.014 g of AIBN (0.085 mmol) under nitrogen was added a solution of MAA (0.22 g, 2.56 mmol) in anhydrous acetone (3 mL) via cannula. The solution was heated under nitrogen at 50 °C with UV irradiation (mercury lamp, 100 W) for 24 h. After polymerization, the polymer was filtered and purified by dissolving in a minimum amount of methanol and re-precipitated in a 10-fold excess of Et_2O solution. The polymer was collected by filtration, washed with Et_2O and dried under vacuum for overnight (0.29 g, yield: 77%). ^{1}H NMR (DMSO-d_6) δ: 0.53–1.33 (m, CH_3– of polymer backbone and HPMA), 1.70 (bs, –CH_2– of polymer backbone), 2.25 (s, CH_3- of oxazole), 2.88 (m, –NH–CH_2– of HPMA), 3.61 (m, –CH_2–CH(CH)$_3$OH of HPMA and –NH–CH_2–CONHCH$_2$– of MA-GG-SMX), 3.90 (bs, –NH–CH_2–CONH–Ar of MA-GG-SMX and –NH–CH_2–CONHCH$_2$– of MA-GG-ONp), 4.07 (bs, –NH-CH_2–COOAr of MA-GG-ONp group), 4.69 (bs, O*H* of HPMA), 6.08 (s, –*H* of oxazole ring), 7.40 (d, ONp–*H*, J = 6.9 Hz), 7.78 (s, Ar–*H* of MA-GG-SMX), 8.28 (d, ONp–*H*, J = 6.9 Hz), 8.39 (m, N*H*–), 10.19 (bs, –N*H*), 11.33 (bs, –N*H*), 12.34 (bs, –COO*H*). ^{13}C NMR (DMSO-d_6) δ: 11.82, 15.73–18.66, 21.99, 42.31, 42.41, 44.07, 47.40, 50.33–55.61, 65.02, 95.68, 119.04, 123.23, 125.23, 127.83, 133.40, 180.02, 142.88, 145.22, 155.21, 157.84, 170.05, 171.23, 177.29. IR (KBr) ν (cm^{-1}): 3410 (N–H), 2993, 2936 (C–H), 1713 (C=O), 1644 (C=O), 1532 (C=C), 1498 (N=O asym), 1382 (S=O asym), 1342 (N=O sym), 1257 (C–O), 1166 (C–O).

2.3.3. Synthesis of N-(4-tert-butoxycarbonyl-aminobutyl) maleimide (**6**)

N-Boc protection of 1,4-diaminobutane was carried out with $(Boc)_2O$ according to the literature [43]. *N*-Boc-protected 1,4-diaminobutane (**4**) (2.37 g, 12 mmol) was added to a solution of maleic anhydride (1.38 g, 14 mmol) in acetone (20 mL) and the reaction mixture was stirred at 5 °C for 1 h. The mixture was dried under reduced pressure and re-dissolved in 20 mL of ethyl acetate. The organic layer was extracted with three portions of water (20 mL), dried over anhydrous magnesium sulfate and concentrated under reduced pressure to give crude *N*-(4-tert-butoxycarbonyl-aminobutyl)maleamic acid (**5**) (2.99 g, yield: 82%). The resulting maleamic acid product (1.23 g, 4.3 mmol) was then heated with sodium acetate (0.37 g, 4 mmol) in acetic anhydride (3.7 mL, 36 mmol) at 100 °C for 1 h. The mixture was cooled to room temperature, washed with excess water to remove most acetic anhydride and the resulting brown oil residue was dissolved in 30 mL of ethyl acetate. The solution was extracted twice with equal volumes of saturated $NaHCO_3$ solution and water until the solution was neutral. The organic layer was dried over anhydrous magnesium sulfate and concentrated under reduced pressure to leave the residue, which was further purified by flash chromatography (silica gel, 90:10 CH_2Cl_2/EtOAc) to afford the white product **6** (0.42 g, yield: 37%). ^{1}H NMR ($CDCl_3$) δ: 1.43 (s, 9H, $-COOC(CH_3)_3$), 1.51–1.62 (m, 4H, $-NHCH_2-(CH_2)_2-CH_2NH-$), 3.11 (m, 2H, $-CH_2-CH_2-NHCOOBu$), 3.54 (t, 2H, $-CH_2-CH_2-$maleimide, J = 7.05 Hz), 4.50 (bs, $-NH$), 6.66 (s, 2H, $-CH=CH-$). ^{13}C NMR ($CDCl_3$) δ: 25.75, 26.98, 28.32, 37.22, 39.60, 79.34, 134.32, 155.83, 170.87.

2.3.4. Synthesis of N-(4-aminobutyl)maleimide(AMI) (**7**)

Trifluoroacetic acid (1.0 mL, 13 mmol) was added to a stirred solution of compound **6** (0.44 g, 1.6 mmol) in anisole (0.2 mL) at room temperature. After stirring for 1 h, the solvent was evaporated under reduced pressure and the resulting residue was dissolved in a minimum amount of ethyl acetate. The solution was added to a 10-fold excess of *n*-hexanes and the product was isolated as a white powder by filtration, rinsed with *n*-hexanes and vacuum-dried for overnight (0.26 g, yield: 96%). ^{1}H NMR (D_2O) δ: 1.48 (m, 4H, $NH_2CH_2-(CH_2)_2-CH_2-$imide), 2.84 (t, 2H, $NH_2-CH_2-CH_2-$, J = 7.05 Hz), 3.38 (t, 2H, $-CH_2-CH_2-$imide, J = 7.05 Hz), 6.68 (s, 2H, $-CH=CH-$). ^{13}C NMR (DMSO-d_6) δ: 24.33, 24.92, 36.65, 38.40, 134.09, 171.03.

2.3.5. Synthesis of poly(MAA-co-HPMA-co-ma-GG-SMX-co-MA-GG-AMI) (**2**)

The AMI (0.01 g, 0.06 mmol) and Polymer **1** (0.10 g) were dissolved in 1.0 mL of anhydrous DMSO and heated to 80 °C under nitrogen for 24 h. The reaction mixture was added to a 10 mL portion of acetone and the polymer was filtered, purified by dissolving in a minimum amount of methanol and re-precipitated into a 10-fold excess of Et_2O solution. The product was isolated as a light-yellow powder by filtration, rinsed with Et_2O and vacuum-dried for overnight (0.06 g, 60%). ^{1}H NMR (DMSO-d_6): δ: 0.53–1.31 (m, CH_3- of polymer backbone and HPMA), 1.33–1.70 (m, $-CH_2-$ of polymer backbone and AMI linker), 2.25 (s, CH_3- of oxazole), 2.88–2.89 (m, $-NH-CH_2-$ of HPMA and $-CONH-CH_2-CH_2-$ of AMI linker), 3.61–3.90 (m, $-CH_2-CH(CH)_3OH$ of HPMA and $-NH-CH_2-CONHCH_2-$ of MA-GG-SMX and AMI groups), 4.69 (bs, OH of HPMA), 6.08 (s, $-H$ of oxazole ring), 6.96 (s, $-CH=CH-$), 7.36 (m, $-NH$), 7.78 (s, Ar$-H$ of MA-GG-SMX), 8.39 (m, $-NH$), 10.19 (bs, $-NH$), 12.34 (bs, $-COOH$). ^{13}C NMR (DMSO-d_6) δ: 11.82, 15.73–18.66, 21.99, 25.80, 26.38, 36.84, 38.22, 42.31, 42.41, 44.07, 47.40, 50.33–55.61, 65.02, 95.68, 119.04, 127.83, 133.40, 142.88, 157.84, 170.05, 171.23, 177.29, 180.02. IR (KBr) – (cm^{-1}): 3406 (N–H), 2998, 2979 (C–H), 1708 (C=O), 1646 (C=O), 1542 (C=C), 1382 (S=O), 1254 (C–O), 1175 (C–O).

2.4. Determination of critical micelle concentration (CMC) of Polymer **1**

4 μL of pyrene stock solution in acetone (1.26 mM) was added to each of a series of 10-mL volumetric flasks and the acetone evaporated. To each flask was then added 10 mL of Polymer **1** solution with various concentration (0.001 mg/mL–2.0 mg/mL). Fluorescence spectra were obtained from 360 to 460 nm following excitation at wavelength of 339 nm. The intensities of excitation peaks at 373 nm and 393 nm were recorded and the ratios were plotted as the function of polymer concentrations.

2.5. Antimicrobial activity test

The antimicrobial activity of Polymer **1** was evaluated against *E. coil* (DH5) using LB broth solutions. Prior to the test, Polymer **1** (0.2 mg) was dissolved with 200 μL of LB broth either in the existence or absence of 4 μL DMSO at different starting pH values (4, 4.5, 5, 5.5, 6, 6.5, 7, 7.5 and 8) to reach a final concentration of 0.1% (w/v).

The bacteria suspension (5 μL, 4×10^4 CFU/mL of *E. coli*) was then added in triplicate into each corresponding media in 96-well culture plates and incubated at 37 °C, 160 rpm for 18 h. Microbial growth was measured as an increase of optical density at 630 nm (OD_{630}) by a microplate reader after incubation and the results of antimicrobial effects were expressed by optical density ratio (treated sample/control sample). The low value of the OD_{630} ratio represents the high level of the antimicrobial efficiency.

2.6. Preparation of Fab′ and F(ab′)$_2$ fragments

The antibody Fab′ and F(ab′)$_2$ fragments were prepared freshly using the Pierce Mouse IgG1 Fab′ and F(ab′)$_2$ Micro Preparation Kit (Thermo Fisher Scientific Inc., Rockford, IL, USA) following the instructions provided with the Kit. Pan CEA (H-8): sc-48364 mouse monoclonal IgG1 antibody in digestion buffer was mixed with immobilized ficin for 24 h at 37 °C to give F(ab′)$_2$ and the undigested IgG was removed on an immobilized Protein A column. The F(ab′)$_2$ was further reduced to Fab′ with 20 mM cysteine (Sigma) in 20 mM Tris–HCl buffer (pH 8.5) for 1 h at 37 °C. The collected fractions containing Fab′ fragments were passed through the column (Amicon Ultra-4) using PBS buffer and stored at 4 °C.

2.7. Solid-phase immunoassay

Nunc F96 MicroWell Plates (Thermo Fisher Scientific Inc., Rockford, IL, USA) were coated with 100 μL Polymer **2** (3 wt % in phosphate-buffered saline, PBS) for 4 days at 25 °C. The arrays were rinsed with PBS and then, 50 μL of Fab, F(ab′)$_2$ and BSA were added in triplicate to each well and incubated for 2 h in the dark at 25 °C. The mean background reactions were evaluated by the BSA test samples. After washing three times with PBS, each well was blocked with 50 μL of BSA for 1 h at room temperature. The blocking solution was removed and the plate was washed successively with PBS and subsequently, 50 μL of HRP-conjugated anti-mouse IgG1 (diluted 1:1000 in PBS) was added. After incubation for 1 h at room temperature, the plate was washed three times with PBS buffer and 50 μL/well TMB substrate was added. Then 2 N HCl (50 μL) was added to each well and the chromogenic reactions were

measured on a microplate reader (PowerWave 340, BioTek) at 450 nm.

3. Results and discussion

3.1. Preparation and characterization

3.1.1. Monomers and Polymer **1**

The tetrapolymer poly(MAA-*co*-HPMA-*co*-MA-GG-SMX-*co*-MA-GG-ONp) (**1**) was synthesized in good yield by radical copolymerization of MAA and HPMA with a polymerizable drug derivative MA-GG-SMX and a reactive monomer MA-GG-ONp, as shown in Scheme 1. The MAA segment in the drug carrier was selected for its ability to respond to pathologic changes of pH and to precipitate in the acidic environment. The HPMA segment was chosen for its non-toxic, biocompatible and hydrophilic nature that can enhance the water solubility of hydrophobic drugs.

MA-GG-ONp was prepared by the reaction of glycylglycine with methacylchloride in an aqueous alkaline solution, followed by esterification with *p*-nitrophenol in the presence of DCC. Scheme 2 shows how the treatment of the ONp ester with SMX in DMF provided the methacryloylglycylglycine derived drug monomer MA-GG-SMX in a 60% yield. The formation of MA-GG-ONp and MA-GG-SMX was confirmed by NMR spectroscopy, as shown in Fig. 1. The ^{1}H NMR spectrum of MA-GG-SMX showed 2 sharp singlet signals at $\delta = 6.09$ ppm and $\delta = 2.28$ ppm (denoted as *l* and *m* in Fig. 1) corresponding to the vinyl and methyl protons of oxazole, respectively. The ^{13}C NMR spectrum also confirmed all carbon resonances of each monomer. Four aromatic protons of MA-GG-SMX appeared as a singlet at 7.78 ppm (denoted as *i* and *j* in Fig. 1), whereas 2 doublet peaks of *p*-nitrophenol ($\delta = 7.42$ and 8.28) were observed on MA-GG-ONp. These differences, in addition to the characteristic resonances of oxazole, were employed to estimate the relative molar concentration of each component.

Fig. 2 shows the representative ^{1}H NMR spectra and the assignment of the resonances of Polymer **1**. The broad resonance peak at 2.7–3.0 ppm (denoted as *g*) was attributed to the methylene protons of HPMA and applied in the molar composition analysis. Subsequently, the molar ratios of each component (denoted as *m*, *n*, *o*, and *p*) were calculated by comparing the average integrals at $\delta = 2.70$–3.10 ppm, 2.25 ppm, and 7.42 ppm (denoted as *g*, *v* and *c*′, respectively), with the peak area of methyl protons at $\delta = 0.53$–1.33 ppm (denoted as *a*, *d*, *i*, *k* and *w*, respectively). The equation is displayed as follows:

$$n = (g/2)/\{[(a+d+i+k+w) - ((g/2)^{*}3)]/3\}$$

$$o = (v/3)/\{[(a+d+i+k+w) - ((g/2)^{*}3)]/3\}$$

$$p = (c'/2)/\{[(a+d+i+k+w) - ((g/2)^{*}3)]/3\}$$

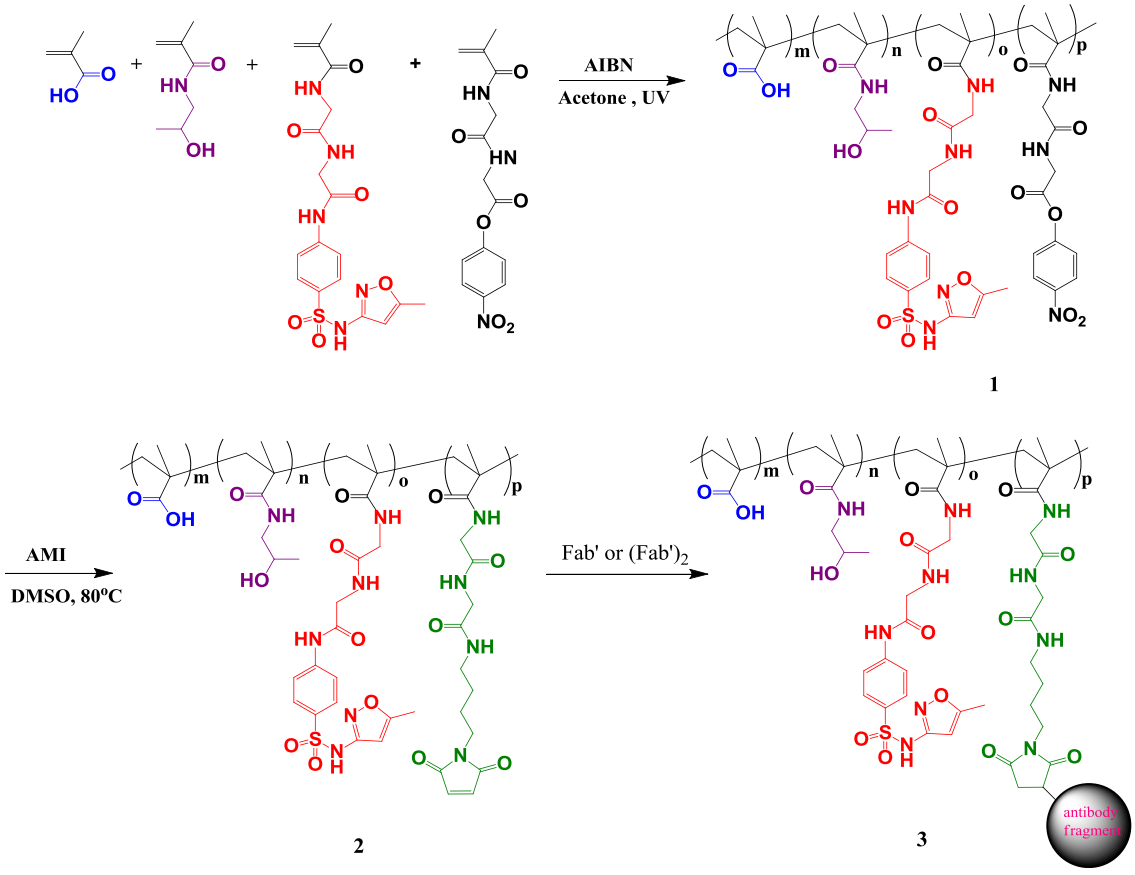

Scheme 1. Synthetic route for the preparation of polymer–drug conjugate.

$m = 1 - n - o - p$

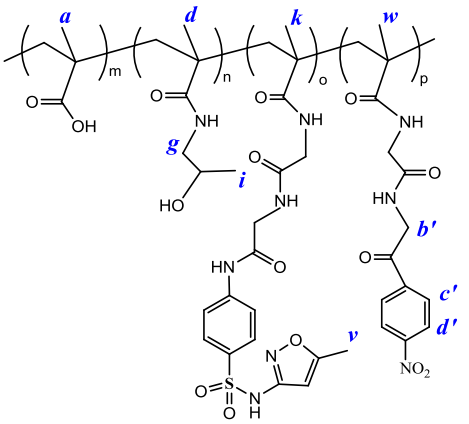

The tetrapolymer was isolated as a light-yellow solid in good yield in acetone, wherein the approximate molar ratio of *m*, *n*, *o* and *p* was 13:2.5:1:1.5 (entry 1, Table 1), respectively. The molar composition, molecular weight and yield varied slightly when polymerizations were carried out in DMF at 50 °C (entry 2). The GPC chromatographs of both polymers showed unimodal peaks of M_n ranging from 8400 to 15,000, with a polydispersity of 1.9–2.5, revealing a smooth radical polymerization obtained under different reaction conditions. Because of the higher yield and molecular weight, the product from entry 1 was used for subsequent reactions.

3.1.2. Linker and Polymer **2**

N-[4-aminobutyl]maleimide (AMI) is a thiol-reactive, non-biodegradable spacer that connects polymers and target ligands, making the antigen-binding site more approachable in pathological areas. AMI synthesis is shown in Scheme 3, where the linker length (C_n) can be modified, if necessary. Initially, the diaminobutane was monoalkylated with $(Boc)_2O$ to yield **5**, which was then reacted with maleic anhydride followed by cyclization with Ac_2O/NaOAc yielding the *N*-Boc-protected aminomaleimide (**6**). Removal of the *N*-Boc group was achieved by treating with TFA to provide the AMI (**7**) in good yield. Then, the linker was incorporated into the side chain by reacting Polymer **1** with AMI in DMSO with the removal of the −ONp group. A representative ^{1}H NMR spectrum of Polymer **2** is shown in Fig. 3. For Polymer **2**, the ^{1}H NMR spectrum exhibits a singlet at $\delta = 6.96$ ppm (vinyl protons of maleimide, denoted as *h*′ in Fig. 3). This, in addition to the concomitant disappearance of the nitrophenol peaks (denoted as *c*′ and *d*′ in Fig. 2), indicated a successful aminolysis reaction. Based on GPC chromatography results, M_n was approximately 18,000, with a polydispersity of 2.9. Presumably, the antibody fragments are capable of conjugating to the polymer by the Michael addition reaction between a sulfhydryl-containing molecule, such as cysteine, and maleimide, thereby forming a thioether bond [44]. In this case, the antibody-mediated targeting of tumor cells could increase the tumor-specific accumulation of drugs. Furthermore, the subsequent precipitation caused by pH changes in the endosome or tumor surface could assist drug accumulation within the tumor cell.

3.2. Stimulus-responsive transition of Polymer **1**

The pH-responsive behavior of Polymer **1** can be described as an ionization level of the polymer in an aqueous solution, resulting in transmittance changes of the solution. Fig. 4 shows the pH-dependent turbidity of the micelle solution. When the solution pH level decreased, the relative transparency of the solution was reduced by 75% at pH levels of 3.5. The cloud point of the polymer solution occurred at pH 6.5–3.5, responding in accordance with the properties associated with the extracellular environment of solid tumors and endocytosis. At normal physiological or higher pH values, the carboxylic acid groups of MAA were ionized and solvated in water. This resulted in the hydrophobic sulfonamide units being embedded within the microspheres, with a diameter ranging from 50 to 150 nm, as shown in the TEM image (Fig. 5a). As the pH decreased, the carboxyl groups of the MAA segments became protonated and intrapolymer chain–chain interactions dominated via intramolecular hydrogen bonding. As a result, the micelles started to collapse and partially precipitated into hydrophobic polymer particles which led to a reduced transparency of the solution (Fig. 4) and certain degree of aggregation (Fig. 5b). This pH-induced phase transition is reversible and may presumably allow the temporary “shield” for drugs during delivery.

The ability of Polymer **1** to form micelles in the aqueous solution was tested by fluorescence spectroscopy using pyrene as a probe. The pyrene was mixed with the polymer solutions of various concentrations, and the emission spectra were recorded. Fig. 6 displays the intensity ratios of the first to the third vibrational band at 373 nm and 393 nm (I_{373} and I_{393}), measured as

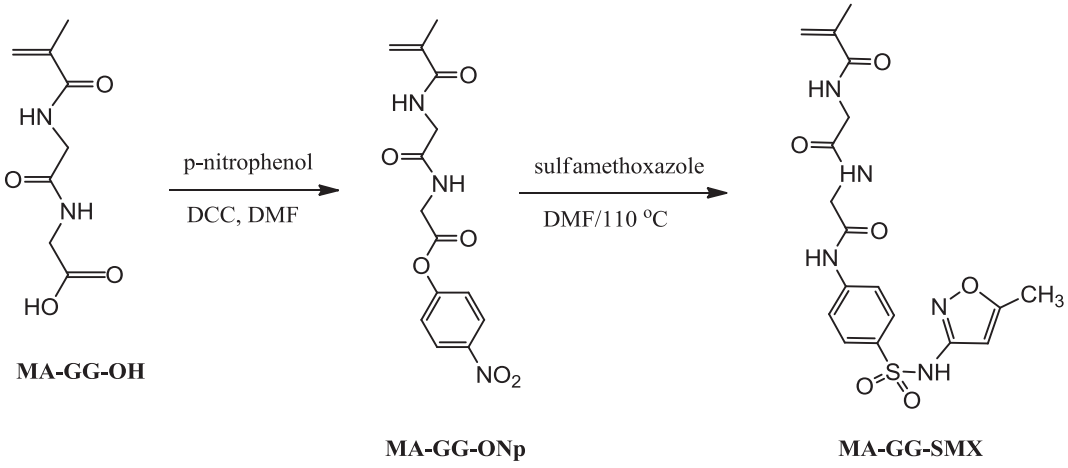

Scheme 2. Preparation of *N*-methacryloyl glycylglycyl sulfamethoxazole.

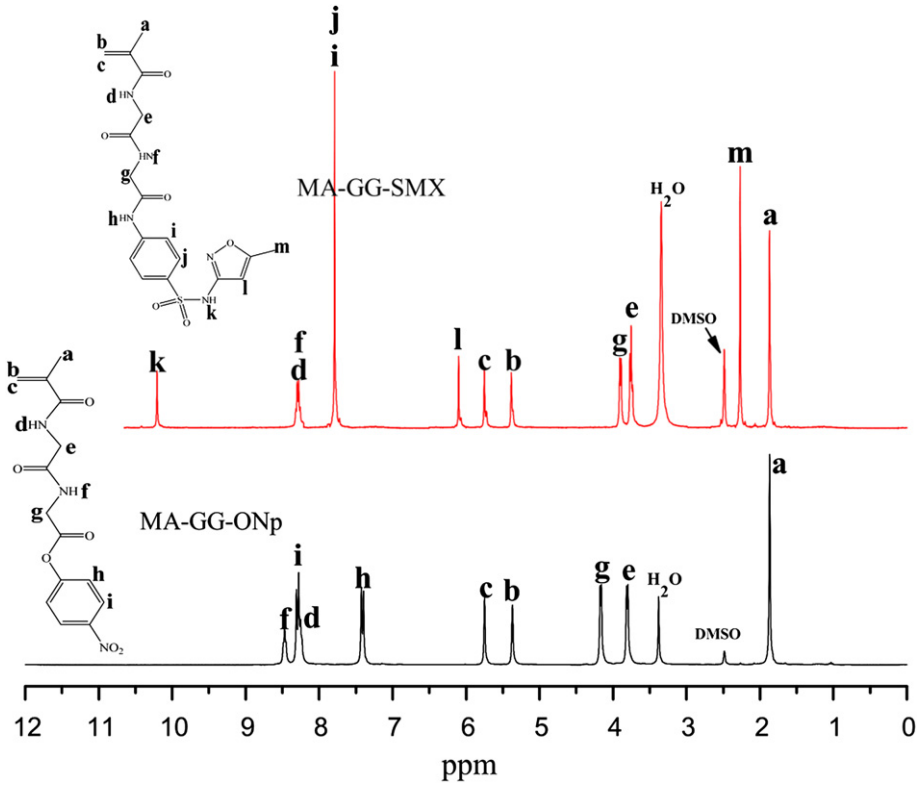

Fig. 1. [1]H NMR spectra of MA-GG-ONp and MA-GG-SMX.

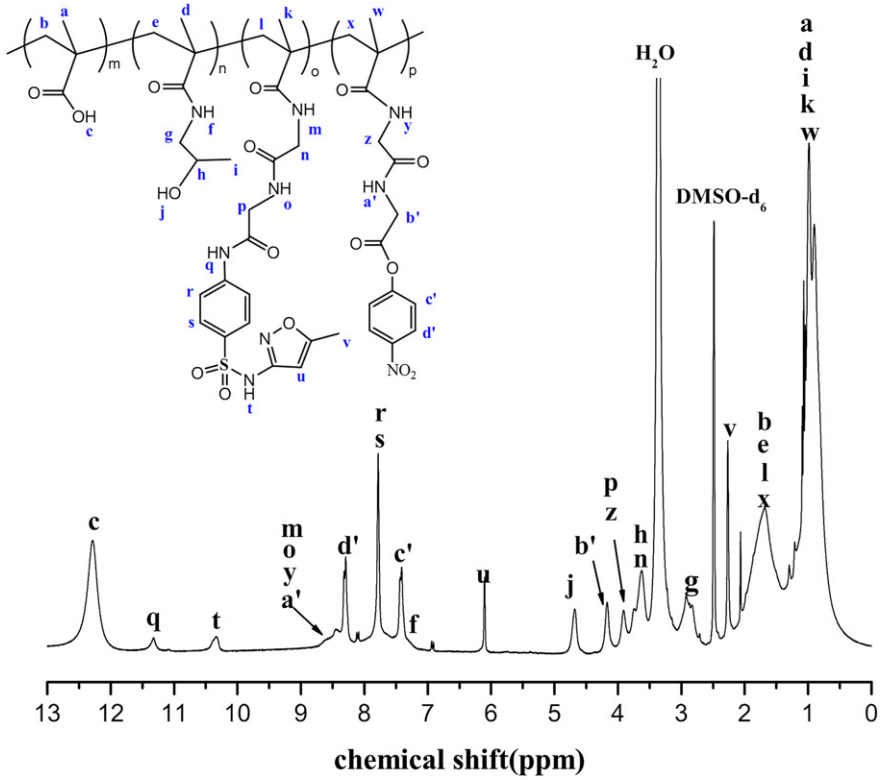

Fig. 2. A representative [1]H NMR spectra of **1**.

Table 1
Reaction conditions and characterization data of Polymer **1**.[a]

Entry	Composition (m:n:o:p)	M_n [b]	M_w [b]	PDI[b] M_w/M_n	$[\eta]$[c] (dL/g)	Temp (°C)	t (h)	Solvent	yield (%)
1	13:2.5:1:1.5	15,085	38,175	2.5	0.12	60	24	Acetone	77
2	17:4:1:1.65	8411	15,927	1.9	0.05	50	24	DMF	50

[a] Feed ratio (mol) m:n:o:p = 16:2:1:1.
[b] Prior to GPC analysis, the polymers were modified by methylation of the carboxylic acid groups using trimethylsilyldiazomethane in DMSO at room temperature.
[c] Intrinsic viscosity ([η]) was measured at 26 °C using Ubbelohde type viscometer in methanol.

a function of polymer concentrations. At low polymer concentrations, I_{373} and I_{393} had a plateau value of approximately 1.3, indicating the absence of polymeric micelles in the solution [45,46]. At concentrations above 1 mg/mL, I_{373} and I_{393} ratios dropped sharply, signaling micelle formation and partitioning of pyrene inside the micelle hydrophobic cores. The critical micelle concentration (CMC) of 1 mg/mL was estimated after the sharp drop in I_{373} to I_{393} ratios.

The solution turned yellow as the pH value increased because of the ionization of the sulfonamide group at a pH higher than its pKa value [47], wherein the deprotonated sulfonamide groups presented intense charge-transfer absorptions at 400 nm, as shown in Fig. 7. The UV–vis spectra of Polymer **1** were recorded from 230 to 600 nm at different pH values in water. The absorptions relative to the phenyl ring in SMX were observed at 270 nm at pH 5.5–6.5. They were reduced with the concomitant appearance of new absorption bands at 400 nm, when the pH of the solution was increased or shifted to 312 nm when the pH level decreased. The development of new bands in the absorption spectra, as well as the change in color of the solution, indicate different charge-transfer interactions between the protonated and deprotonated forms of the sulfonamide group. These results are in accordance with pKa_1 and pKa_2 values of sulfonamide derivatives, as reported by Sanli et al. [48].

3.3. Conjugation of antibody fragments

The conjugation between the antibody fragments and the polymers is evaluated by the solid-phase immunoassay. Antibody fragments (such as Fab′ or $(Fab')_2$) are an attractive alternative to intact mAbs for antibody attachment because of more efficient antigen binding and a simpler structure that provides greater control of the structures of polymer conjugates [49]. The antibody fragments Fab′ and $(Fab')_2$ were prepared from the pan CEA (H-8) antibody: sc-48364 mouse monoclonal IgG1 antibody according to supplier's protocol. This carcinoembryonic antigen is capable of examining various cancer diseases [50]. Polymers **1** and **2** were pre-coated onto Nunc F96 MicroWell plates. Prior to use, each well was treated with BSA, and Fab′ and $(Fab')_2$ fragments for conjugation. The plate was washed thoroughly with PBS, and then the secondary antibody and chromogenic substrate were added. The test samples were analyzed on the microplate reader at 450 nm. For Polymer **2**, the optical density values for the BSA, Fab′ and $(Fab')_2$ were 0.152, 0.353, and 0.861, respectively, with positive-to-negative (P/N) ratios of 2.32 for Fab′ and 5.37 for $(Fab')_2$, indicating successful attachment of both antibody fragments. As a result, the thiol groups of cysteine and primary amine groups of lysine in antibody fragments both could undergo Michael addition, forming the polymer bioconjugate. Polymer **1**

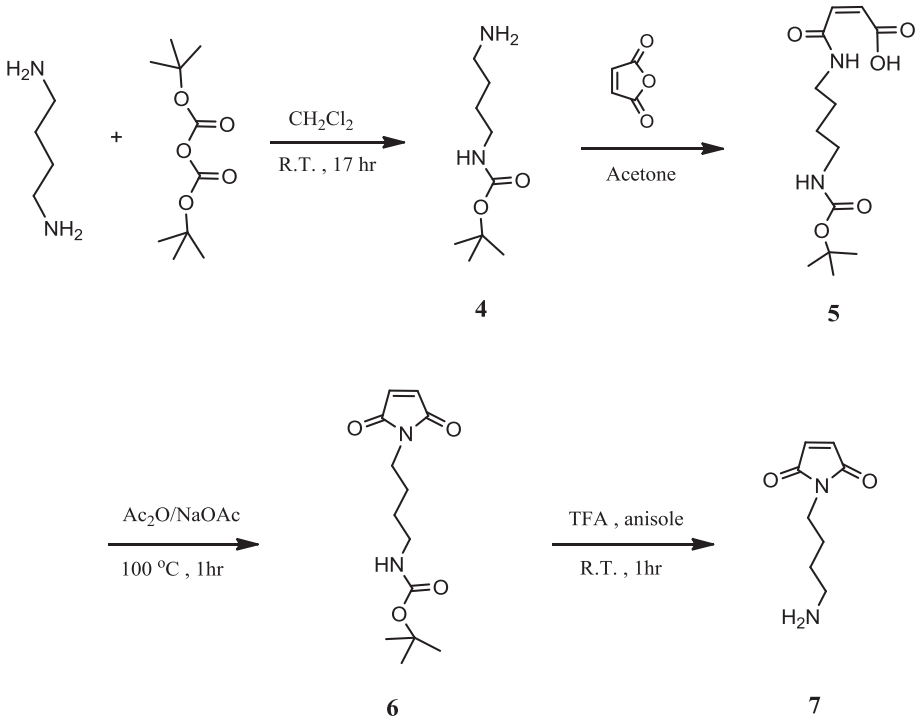

Scheme 3. Preparation of *N*-(4-aminobutyl)maleimide (AMI, **7**).

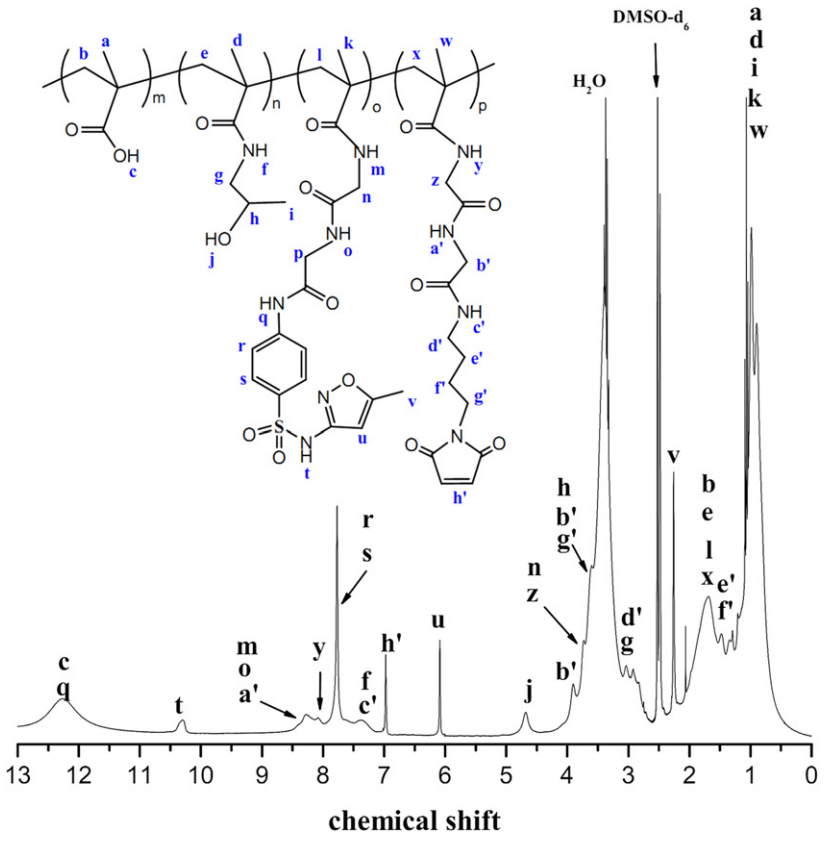

Fig. 3. A representative ^{1}H NMR spectra of **2**.

was also found to be conjugated to Fab′ and $(Fab')_2$ with P/N ratios of 3.12 and 7.23, respectively. This study argues that, because of excellent reactivity of primary amine groups toward a nucleophilic attack, antibody fragments could replace −ONp groups.

3.4. Antibacterial activities

The growth inhibiting effect of Polymer **1** and its structural analog poly(MAA-*co*-HPMA-*co*-MA-GG-ONp) against *E. coli* was evaluated by the survival ratio in the medium containing the polymer and *E. coli* cells. The capability to inhibit the growth of the tested microorganisms (denoted as OD) at different pH media is shown in Fig. 8. Compared with the control sample, both polymers reduced bacterial viability by approximately 10%–20% at a pH level of 4–8 in LB broth media. Furthermore, both polymers had no appreciable difference in antibacterial activity. Albeit adding a small amount of DMSO (2 vol%) not having any major effect on the activity of the tertpolymer (without drug units), it reduced viability (50%–60%) of Polymer **1** significantly. These drastic changes in the antimicrobial activity could be explained by greater solvation ability, thereby the hydrophobic units and the sulfonamide groups embedded inside became more exposed to the test bacteria under culture conditions. Although further investigations are necessary to elucidate the antibacterial mechanism against *E. coli*, the intrinsic activity of the tertpolymer can be partially attributed to the glycine units, which are known to exert antibacterial effect against *E. coli* [51,52].

Growth inhibition was also found to decrease as the pH value increased. The decreased antimicrobial activity at higher pH levels could be accounted for by the polymer's ionization in the basic

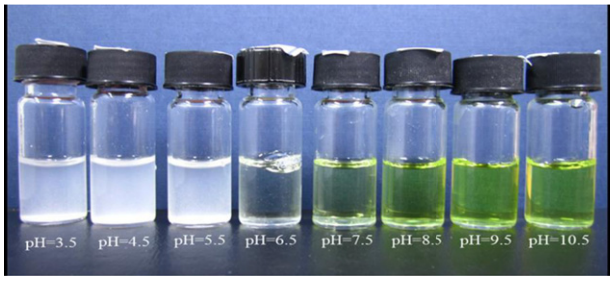

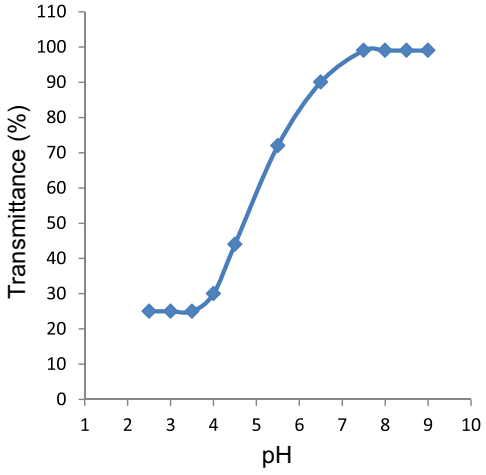

Fig. 4. Transmittance changes of Polymer **1** aqueous solution as a function of pH measured at 600 nm.

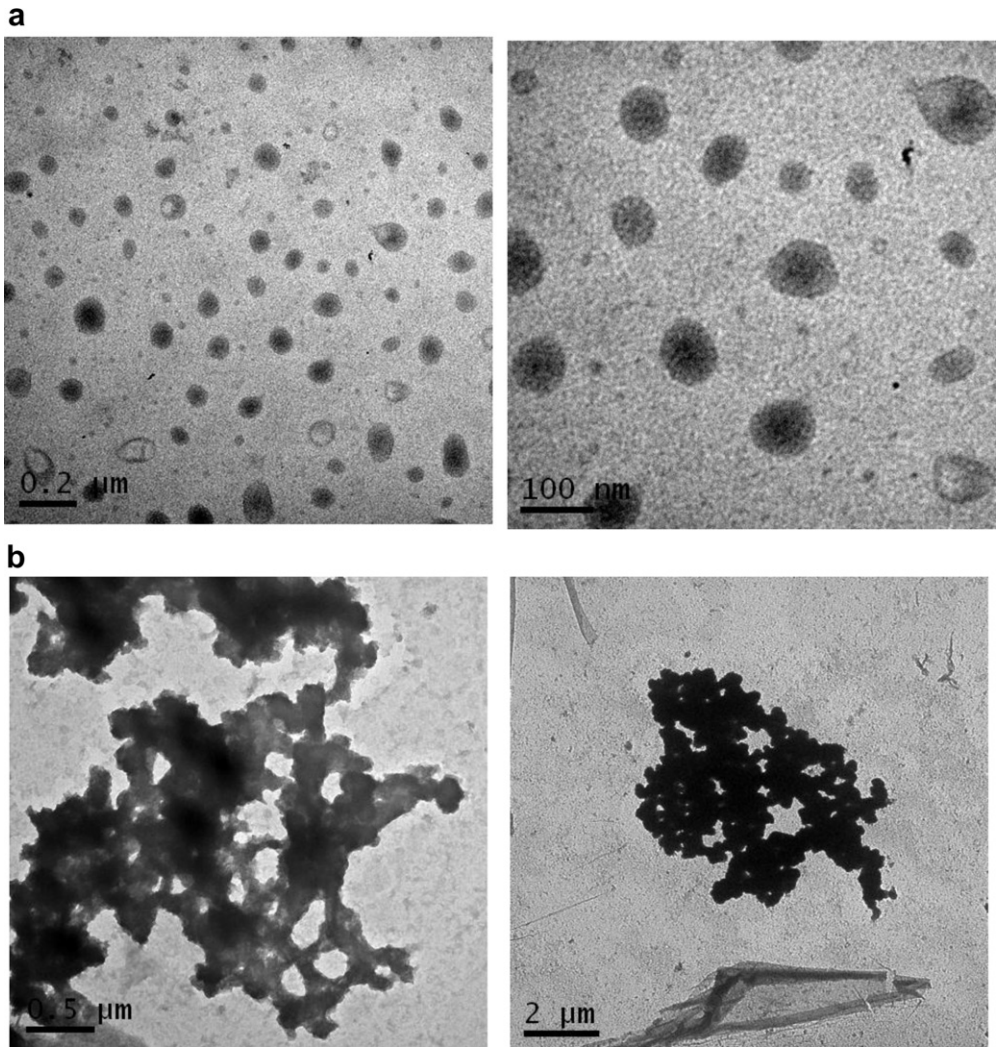

Fig. 5. TEM images of Polymer **1** at a polymer concentration of 1 mg/mL in aqueous solution; (a) pH = 7.5, and (b) pH = 5.5.

solution, wherein fully ionized polymers interact less favorably with the negatively charged *E. coli* outer membrane [53], thereby exhibiting the least antimicrobial activity at pH 8. The in vitro results are promising because they indicate that appropriate polymer aggregation in the specific situation can increase the effectiveness of the drug and facilitate its contact with acidic surfaces. Further studies are in progress for replacing SMX with other anti-cancer drugs (doxorubicin, epirubicin, and gemcitabine) and its effects on antitumor activity.

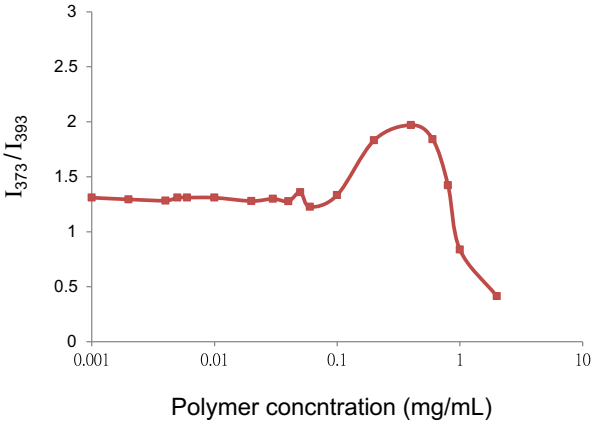

Fig. 6. Relation between intensity ratio (I_{373}/I_{393}) of pyrene emission spectra (λ_{ex} = 339 nm) and Polymer **1** concentration at pH = 7.5, 25 °C.

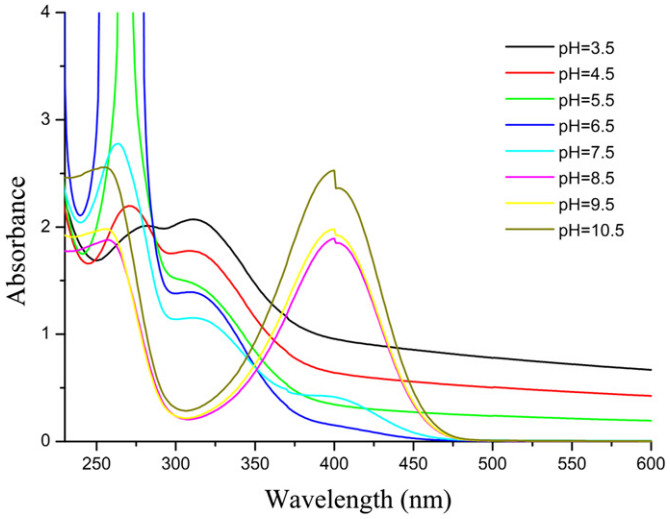

Fig. 7. UV–vis spectra of Polymer **1** at different pH levels.

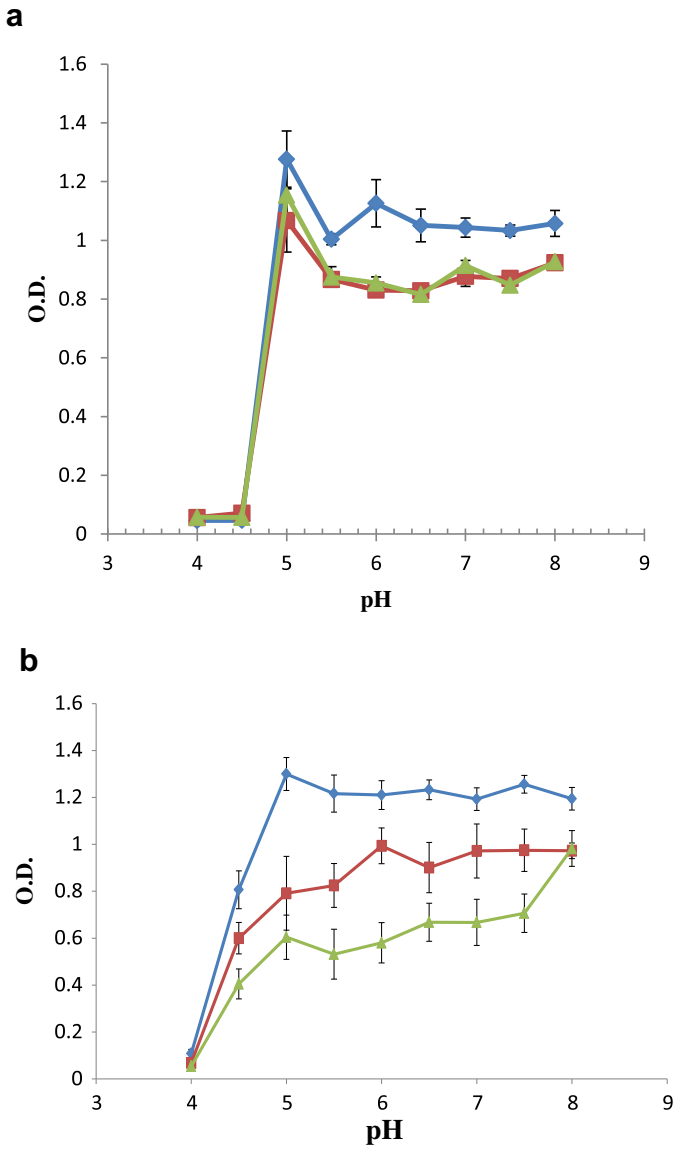

Fig. 8. Growth inhibition of *E. coli* control (◆), Polymer **1** (▲) and poly(MAA-*co*-HPMA-*co*-MA-GG-ONp) (■) for 18 h at 37 °C, 160 rpm at different pH levels in (a) in LB broth media and (b) DMSO-mediated LB broth media.

4. Conclusions

This research developed a water-soluble drug delivery system capable of carrying tumor-specific targeting moieties and activating drug precipitation processes under acidic conditions. The fluorescence spectra and TEM image showed that Polymer **1** self-assembled to form a spherical micelle with a diameter ranging from 50 to 150 nm at pH 7.5. Altering the pH of the solution leads to a different extent of aggregation at pH 6.5–3.5, in accordance with the properties associated with the extracellular environment of solid tumors and endocytosis. Because of the solvation and ionization effects, Polymer **1** showed considerably enhanced antibacterial activities against *E. coli* in the presence of DMSO, and the growth inhibition decreased as the pH value increased. The chemical structures of Polymers **1** and **2** are well-characterized and both polymers successfully conjugated with antibody fragments. Theoretically, a number of antitumor polymer–drug conjugates could be altered with the replacement of different drug molecules and conjugated to relevant homing device. Such conjugates demonstrate the feasibility of combining pH sensitivity and bio-selectivity that facilitate site-specific accumulation and possess a high potential for designing new multifunctional antitumor drug delivery systems.

Acknowledgment

Financial supports from National Science Council (NSC 99-2113-M-415-010-MY3) of Taiwan, R.O.C. is gratefully acknowledged.

References

[1] Maeda H, Greish K, Fang J. Adv Polym Sci 2006;193:103–21.
[2] Greish K, Nagamitsu A, Fang J, Maeda H. Bioconjug Chem 2005;16:230–6.
[3] Gabizon AA. Cancer Invest 2001;19:424–36.
[4] Lutz J, Börner HG. Prog Polym Sci 2008;33:1–39.
[5] Minko T. Drug Discov Today Tech 2005;2:15–20.
[6] Li C, Wallace S. Adv Drug Deliv Rev 2008;60:886–98.
[7] Park JH, Lee S, Kim J, Park K, Kim K, Kwon IC. Prog Polym Sci 2008;33:113–37.
[8] Klok HA. J Polym Sci Part A Polym Chem 2005;43:1–17.
[9] Li C. Adv Drug Deliv Rev 2002;54:695–713.
[10] Larson N, Ghandehar H. Chem Mater 2012;24:840–53.
[11] Maeda H, Bharate GY, Daruwalla J. Eur J Pharm Biopharm 2009;71:409–19.
[12] Iyer AK, Khaled G, Fang J, Maeda H. Drug Discov Today 2006;11:812–8.
[13] Duncan R. Nat Rev Drug Discov 2003;2:347–60.
[14] Duncan R. Nat Rev Cancer 2006;6:688–701.
[15] Putnam D, Kopeček J. Adv Polym Sci 1995;122:55–123.
[16] Kovář M, Strohalm J, Etrych T, Ulbrich K, Říhová B. Bioconjug Chem 2002;13:206–15.
[17] Omelyanenko V, Kopecková P, Gentry C, Shiah JG, Kopeček J. J Drug Target 1996;3:357–73.
[18] Říhová B, Kopečková P, Strohalm J, Rossmann P, Větvička V, Kopeček J. Clin Immunol Immunopathol 1988;46:100–14.
[19] Auditore-Hargreaves K, Houghton RL, Monji N, Priest JH, Hoffman AS, Nowinski RC. Clin Chem 1987;33:1509–16.
[20] Monji N, Hoffman AS. Appl Biochem Biotechnol 1987;14:107–19.
[21] Brannon-Peppas L, Blanchette JO. Adv Drug Deliv Rev 2004;56:1649–59.
[22] Kohler G, Milstein C. Nature 1975;256:495–7.
[23] Sudimack J, Lee RJ. Adv Drug Deliv Rev 2000;41:147–62.
[24] Hilgenbrink AR, Low PS. J Pharm Sci 2005;94:2135–46.
[25] Bellocq NC, Pun SH, Jensen GS, Davis ME. Bioconjug Chem 2003;14:1122–32.
[26] Sahoo SK, Labhasetwar V. Mol Pharmacol 2005;2:373–83.
[27] Dharap SS, Qiu B, Williams GC, Sinko P, Stein S, Minko T. J Control Release 2003;91:61–73.
[28] Xu P, Van Kirk EA, Zhan Y, Murdoch WJ, Radosz M, Shen Y. Angew Chem Int Ed 2007;46:4999–5002.
[29] Ulbrich K, Subr V. Adv Drug Deliv Rev 2004;56:1023–50.
[30] Sethuraman VA, Bae YH. J Control Release 2007;118:216–24.
[31] Lee ES, Na K, Bae YH. Nano Lett 2005;5:325–9.
[32] June RK, Gogoi K, Eguchi A, Cui XS, Dowdy SF. J Am Chem Soc 2010;132:10680–2.
[33] Wadia JS, Dowdy SF. Adv Drug Deliv Rev 2005;57:579–96.
[34] Vivès E, Schmidt J, Pèlegrin A. Biochim Biophys Acta 2008;1786:126–38.
[35] Kratz F, Beyer U, Roth T, Tarasova N, Collery P, Lechenault F, et al. J Pharm Sci 1998;87:338–46.
[36] Beyer U, Roth T, Schumacher P, Maier G, Unold A, Frahm AW, et al. Med Chem 1998;41:2701–8.
[37] Drevs J, Hofmann I, Marme D, Unger C, Kratz F. Drug Deliv 1999;6:89–95.
[38] Tomlinson R, Heller J, Brocchini S, Duncan R. Bioconjug Chem 2003;14:1096–106.
[39] Kopeček J, Bazilova H. Eur Polym J 1973;9:7–14.
[40] Hashimoto N, Aoyama T, Shioiri T. Chem Pharm Bull 1981;29:1475–8.
[41] Couvreur L, Lefay C, Belleney J, Charleux B, Guerret O, Magnet S. Macromolecules 2003;36:8260–7.
[42] Rejmanova P, Labsky J, Kopeček J. Makromol Chem 1977;178:2159–68.
[43] Krapcho AP, Kuell CS. Synth Commun 1990;20:2559–64.
[44] Smyth DG, Blumenfeld OO, Konigsberg W. Biochem J 1964;91:589–95.
[45] Kalyanasundaram K, Thomas JK. J Am Chem Soc 1977;99:2039–44.
[46] Ringsdorf H, Venzmer J, Winnik FM. Macromolecules 1991;24:1678–86.
[47] Kang SI, Bae YH. J Control Release 2002;80:145–55.
[48] Sanli S, Altun Y, Sanli N, Alsancak G, Beltran JL. J Chem Eng Data 2009;54:3014–21.
[49] Pedley RB, Boden JA, Boden R, Begent RHJ, Turner A, Haines AMR, et al. Br J Cancer 1994;70:1126–30.
[50] Hance KW, Zeytin HE, Greiner JW. Mutat Res 2005;576:132–54.
[51] Baumann T, Kämpfer U, Schürch S, Schaller J, Largiadér C, Nentwig W, et al. Cell Mol Life Sci 2010;67:2787–98.
[52] Hammes W, Schleifer KH, Kandler OJ. Bacteriol 1973;116:1029–53.
[53] Sonohar R, Muramatsu N, Ohshima H, Kondo T. Biophys Chem 1995;55:273–7.